Supplementary Material

Analysis of Gold in Mineral Ores based on a Newly-built Portable Handheld LIBS System

Chenyu Cao[1#], Changqing Liu[1#], Yiheng Liu[1], Tianwei Wang[1], Mingyu Su[1], Huicong Tao[1], Qibin Zhang[2,3], Zhongyi Bao[2, 3], Zhengjiang Ding[1, 2, 3*], Zongcheng Ling[1]

[1] Shandong Provincial Key Laboratory of Optical Astronomy & Solar-Terrestrial Environment, School of Space Science and Technology, Institute of Space Sciences, Shandong University, Weihai 264209, China.

[2] No.6 Geological Team of Shandong Provincial Bureau of Geology and Mineral Resources

[3] Technology Innovation Center for Deep Gold Resources Exploration and Mining, Ministry of Natural Resources

# These authors contributed equally: Chenyu Cao, Changqing Liu

Corresponding author: Zongcheng Ling (zcling@sdu.edu.cn), Zhengjiang Ding (ytdzhj@126.com)

1. Data processing and model comparison

1.1 Data processing

The data acquired by the PH-LIBS system underwent a two-stage preprocessing procedure: (1) wavelet-based denoising to suppress instrumental white noise, and (2) continuous background subtraction. Figure S1 illustrates the LIBS spectra before and after preprocessing. Comparisons of emission lines confirm that no additional artifacts or distortions were introduced during preprocessing.

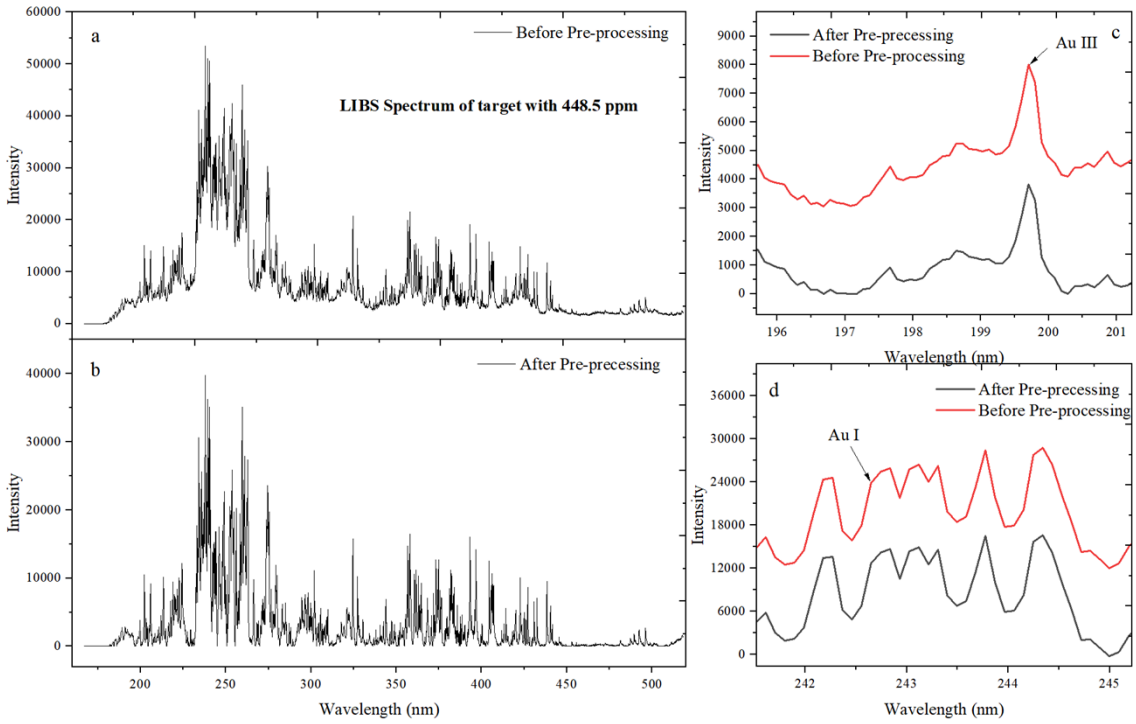

Figure S1 Spectral comparisons before and after Pre-processing. a and b display the spectra of a sample containing 448.5 g/t of gold before and after pre-processing. c and d highlight the changes in the Au spectral peaks at 199.7 nm and 242.8 nm, respectively, resulting from the pre-processing.

1.2 Model comparison

To justify the selection of the random forest (RF) classifier, a systematic comparison was conducted among four machine learning algorithms: RF, support vector machine (SVM), k-nearest neighbor (KNN), and logistic regression (LR).

All classifiers were evaluated under an identical experimental protocol to ensure a fair comparison. The full dataset (n = 108, after removal of the outlier sample at 448 g/t) was partitioned into a training set (80%, n = 86) and an independent held-out test set (20%, n = 22) using stratified random splitting with a fixed random seed (seed = 42). Stratification ensured that the class distribution of low- (<13.3 g/t), medium- (13.3–50 g/t), and high-grade (>50 g/t) samples was preserved in both partitions. The test set was withheld entirely from all training and hyperparameter selection procedures.

Hyperparameter optimization for each classifier was performed exclusively on the training partition using exhaustive grid search (GridSearchCV) combined with 5-fold

stratified cross-validation, preventing data leakage from the test set.

The classification performance metrics for all evaluated models on the independent test set are presented in Table S1. The RF classifier achieved the highest cross-validation accuracy (76.9%), the highest test set accuracy (81.8%), and the highest weighted F1-score (0.811), demonstrating consistent generalization performance. The SVM yielded the lowest test accuracy (72.7%) and weighted F1-score (0.717) among all classifiers, indicating poor generalization on this dataset. Although KNN achieved a comparable test accuracy (77.3%), its training accuracy was 100% with the largest overfitting gap (+0.227), indicating that the model memorized the training samples rather than learning generalizable spectral patterns — a critical concern given the limited dataset size. Logistic regression exhibited stable but lower performance (weighted F1-score = 0.770), likely reflecting the inherently non-linear relationship between Au spectral features and concentration grade levels.

Table S1 classification performance of four machine learning classifiers for Au concentration grading from handheld LIBS spectra. All models were evaluated on the independent 20% held-out test set (n = 22).

Classifier	CV Acc.	Train Acc.	Test Acc.	Weighted F1	Overfitting Gap
RF	76.9%	100.0%	81.8%	0.811	+0.182
SVM	75.5%	83.7%	72.7%	0.717	+0.110
KNN	75.6%	100.0%	77.3%	0.773	+0.227
LR	73.3%	76.7%	77.3%	0.770	-0.005

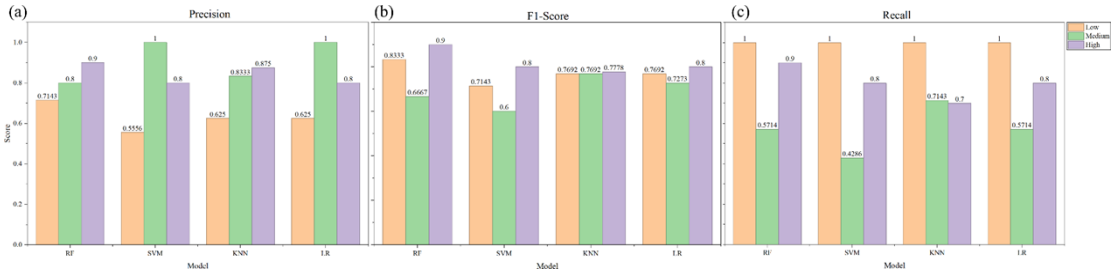

Figure S2 Per-class Precision, Recall, and F1-Score of four classifiers on the independent test set. Grade classes: Low (<13.3 g/t), Medium (13.3–50 g/t), High (>50 g/t).

2. Sample composition

2.1 Sample XRF test results

The analyzed samples, originating from diverse gold mining districts, were processed into certified national reference materials (GBW) through standardized crushing and grinding procedures. Their gold content reflects the natural composition of primary ores, without artificial enrichment.

The abundance of other elements (Table S2) in all samples is confirmed by X-ray fluorescence (XRF). These samples have high Fe (20.62–35.15%) and S (up to 48.69%) contents, along with significant enrichment in Cu, Pb, and Zn, but correspondingly lower SiO_2 abundance (8.05–37.11%). Such elemental distributions align with the geochemical profiles of skarn-type, polymetallic sulfide-type, or gold-bearing pyrite ores.

Table S2 XRF analysis results of gold ore samples

//	Fe	S	Pb	Zn	Cu	SiO_2	Al_2O_3	MgO	CaO	Na_2O	K_2O	Mn	P_2O_5	TiO_2
	%	%	%	%	%	%	%	%	%	%	%	%	%	%
GBW(E)070140	29.01	40.19	0.26	1.39	0.33	19.32	3.98	0.590	1.520	0.310	2.170	0.10	0.08	0.453
GBW(E)070142	35.15	48.69	1.75	0.26	0.57	8.05	3.13	0.360	0.200	0.503	0.711	0.01	0.03	0.079
GBW(E)070143	22.94	30.77	1.05	0.22	0.81	32.25	5.83	0.764	1.584	0.630	2.666	0.04	0.05	0.128
GBW(E)070272	20.62	23.36	0.06	0.08	1.23	37.11	8.33	1.306	2.029	0.625	3.619	0.07	0.10	0.483
GBW(E)070273	24.14	33.97	5.23	3.81	2.17	15.14	6.21	1.570	4.882	0.846	0.919	0.10	0.16	0.299

2.2 Sample microscopic image analysis

At the microscale, however, gold is often distributed heterogeneously. As illustrated in Figure S3, native gold typically occurs as discrete grains irregularly dispersed within the host matrix. When analyzed using laser ablation, the spatial resolution is limited to the diameter of the laser spot (100 μm). If one or more gold grains are present within the ablation area, the resulting measurement can yield a locally elevated gold concentration. This phenomenon reflects the actual microscale distribution of gold rather than an anomalous detection. Despite the instrument's detection limit of 13.3 g/t, it is sufficiently sensitive to capture the presence of gold mineralization at this spatial scale.

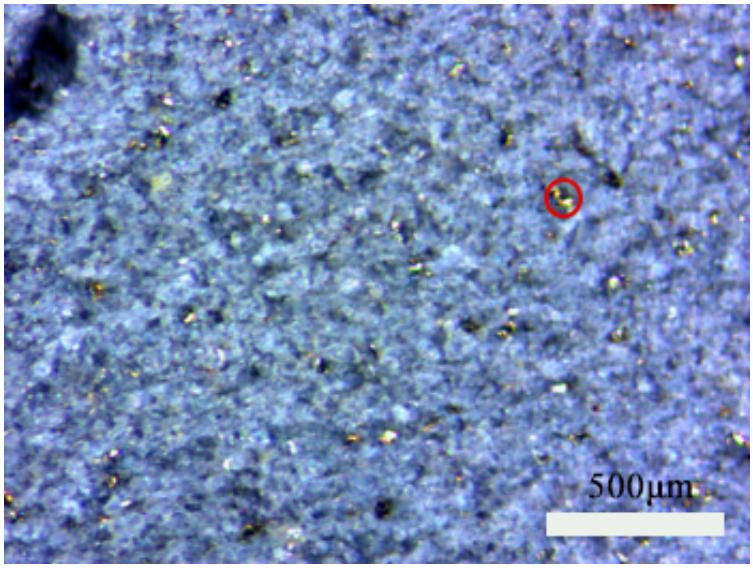

Figure S3 The micrograph of gold ore sample.

2.3 Instrument

Figure S4a illustrates that the PH-LIBS system comprises a laser output unit, a laser control unit, a focusing lens, a spectrometer unit, a compact tablet computer unit, and a protective shell. A laser beam is emitted from the front end of the output unit to excite the target sample, generating plasma. The resulting emission is collected by the focusing lens and transmitted via an optical fiber to the spectrometer unit for spectral processing. As illustrated in Figure S4b, the system features a compact, highly integrated design that facilitates transport and provides sufficient portability and usability for field applications.

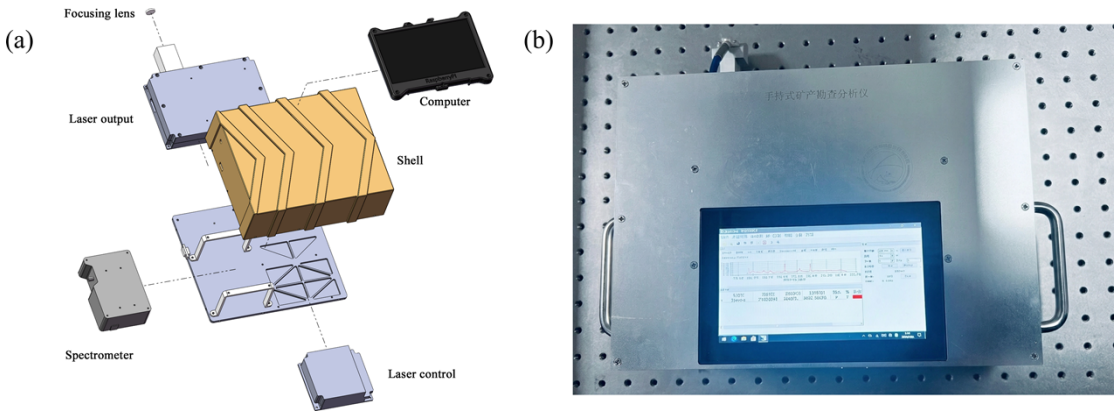

Figure S4 (a) Schematic diagram of the PH-LIBS system components, (b) Real image of PH-LIBS

2.4 SNR Variability at 10 g/t and Justification of the 13.3 g/t LOD

To evaluate detection reliability below the reported empirical LOD (13.3 g/t), three independent LIBS spectral acquisitions were obtained from a 10 g/t certified gold ore reference standard. The resulting SNR values were 3.52, 2.47, and 3.53 (Figure S5). Because one acquisition yielded an SNR < 3, the Au signal at 10 g/t is not consistently detectable. This variability is attributed to the irregular spatial distribution of micro-scale Au grains (i.e., the nugget effect), which causes shot-to-shot fluctuations when the concentration is near the instrument's sensitivity limit.

Consequently, detection at 10 g/t lacks the reproducibility required for a reliable LOD. In contrast, the 13.3 g/t sample consistently exhibited an SNR = 7.44, remaining well above the 3σ threshold. However, the true detection threshold likely falls between 10 and 13.3 g/t. Designating 13.3 g/t as the LOD reflects the lack of certified standards in this intermediate range, rather than a fundamental limitation of the instrument.

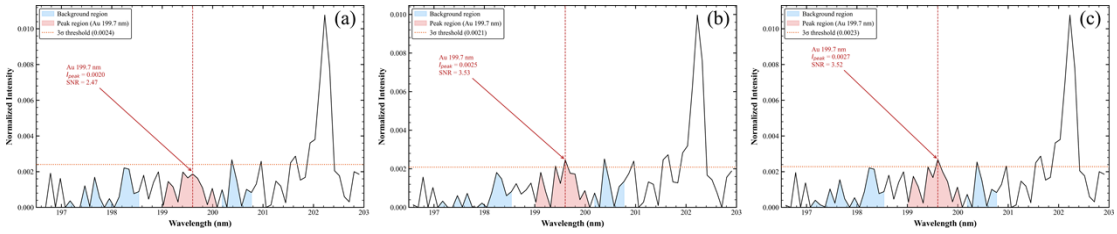

Figure S5 SNR analysis of the Au 199.7 nm emission line in three independent LIBS spectral acquisitions from the 10 g/t gold ore reference standard, displayed over the 196.5–203 nm spectral range.